AAS-22-126

TRAJECTORY PLANNING FOR A PROXIMITY OPERATIONS FLYBY OPERATION ON THE TENZING MISSION

Zachary Burkhardt,[i] Ethan Spessert,[i] Stephen West,[ii] Sergio Gallucci,[iii] Aiden O'Leary,[i] James Bultitude,[i] and Daniel Faber[i]

Safe execution of close proximity operations between two spacecraft is critical to the development of refueling, satellite inspection, and servicing technologies. Previous missions successfully implementing proximity operations and formation flight have done so as a primary mission objective with extensive technology development campaigns and single-use mission planning procedures. This approach is not viable in future widespread refueling and servicing activities where safe proximity operations will not be the primary objective of missions, but rather one phase amongst many in their life cycle. To enable this transition, it is necessary to demonstrate the possibility of implementing proximity operations maneuvers with spacecraft developed using primarily commercial off the shelf (COTS) components with a scalable and adaptable mission planning and operations framework. For these reasons, a proximity flyby operation is planned for the Tanker-001 Tenzing mission. Tanker-001 is the world's first orbital propellant tanker: a ~35 kg small satellite that in addition to its primary mission, serves as an on-orbit testbed for key technologies enabling on-orbit refueling, including Orbit Fab's Rapidly Attachable Fluid Transfer Interface (RAFTI), the SCOUT-Vision stereo imaging, processing, and relative navigation system by SCOUT, and a Benchmark Space Systems HTP (High Test Peroxide) monopropellant thruster system. Successful completion of this flyby activity will demonstrate the feasibility of implementing close proximity operations as a secondary mission objective with SmallSats using COTS components and pave the way for future widespread refueling and inspection activities involving proximity maneuvers.

INTRODUCTION

Emerging game-changing technologies for on-orbit servicing, assembly, and manufacturing (OSAM) will dramatically change the paradigm within the space industry. OSAM missions will enhance the capabilities of spacecraft for existing mission scenarios and enable new mission scenarios. On-orbit refueling and inspection are two OSAM use cases that stand out as they increase the viability and repeatability of other OSAM missions in addition to being valuable stand alone services in their own right.

[i] Orbit Fab, Inc., Denver, CO
[ii] Space Exploration Engineering, LLC, Laurel, MD
[iii] SCOUT Inc., Alexandria, VA

M. Sandnas, D. B. Spencer (eds.), *Proceedings of the 44th Annual American Astronautical Society Guidance, Navigation, and Control Conference, 2022*, Advances in the Astronautical Sciences 179, https://doi.org/10.1007/978-3-031-51928-4_68

On-orbit refueling will enable new mission concepts and help extend the operational lifetimes of space assets[1]. Missions will no longer be constrained by the limitations imposed by the amount of propellant they carry at launch, driving new approaches to spacecraft design and operations. This results in significant cost and schedule savings. One spacecraft can complete repeated or extended missions, saving costs and schedule delays for asset replacement. Spacecraft can also be launched with less initial fuel supply and refuel later, saving on system size, complexity, and launch cost. Access to fuel on-orbit also offers enhanced flexibility; with refueling available, spacecraft operators can more easily elect to reposition assets based on changing operational circumstances. Additionally, refueling increases the efficiency and availability of other OSAM activities by enabling complex servicing vehicles to operate longer and serve more clients over a wider variety of orbits[2].

Refueling, inspection, and other OSAM activities depend on safe and reliable rendezvous and proximity operations (RPO) maneuvers and systems. RPO has been implemented successfully on-orbit numerous times dating back to the Gemini missions in the 1960s. However, these successes have typically been the result of extensive and costly development programs dedicated to ensuring success within the context of that particular mission scenario. This approach is not compatible with widespread implementation of OSAM. Future missions providing or receiving OSAM services will need to complete RPO frequently in a wide variety of scenarios; these RPO activities will be routine enablers of mission objectives rather than being a primary focus of mission design. This will necessitate an approach to RPO that can be implemented with lower costs, faster schedules, and flexible, safe maneuver plans.

To bridge this gap between legacy RPO development approaches and what is necessary for future OSAM missions, Orbit Fab, SCOUT, and Space Exploration Engineering have partnered to implement an RPO flyby as a secondary mission for Orbit Fab's Tanker-001 Tenzing spacecraft. This paper outlines the approach used for maneuver planning for this operation. First, the paper provides a general overview of the Tenzing mission. Next, the paper elaborates on the motivations for this flyby operation in the context of RPO needs for future OSAM missions. Then, the paper details the trajectory design for the flyby and the process used for maneuver planning.

TENZING MISSION OVERVIEW

Launched in June 2021, Tanker-001 Tenzing made history as the world's first orbital propellant tanker[3]. Tenzing is a small satellite built on an Astro Digital bus with the primary mission of carrying a supply of High Test Peroxide (HTP) monopropellant and storing it in orbit. The Tenzing mission is making tangible strides towards the vision of widespread OSAM activities including refueling and inspection by demonstrating the propellant tanker concept and by serving as an orbital testbed for game-changing technologies which will enhance the capabilities, availability, and reliability of these services. Figure 1 shows the Tenzing spacecraft with key payloads highlighted. Tenzing's design approach also emphasized the use of COTS components to facilitate the development and proliferation of these technologies on a rapid schedule with low cost.

Tenzing's primary mission is fulfilled by the Primary Tank payload developed by Orbit Fab. This tank carries Tenzing's HTP supply and includes instrumentation for pressure monitoring and thermal control. The primary tank was filled using Orbit Fab's Rapidly Attachable Fluid Transfer Interface (RAFTI). RAFTI is a fill-drain valve for spacecraft propellant systems and an interface for on-orbit grappling/attachment and fuel transfer[4].

Local situational awareness capabilities and remote sensing are provided by the on-board spacecraft vision payload, SCOUT-Vision. This system delivered by SCOUT is a stereoscopic imaging system which includes on-board processing power to enable real-time data gathering and

analytics. SCOUT-Vision provides a combination of imagery and derivative data products, e.g. pointing information, state estimation of resident space objects (RSOs), and relative navigation information with regards to RSOs.

Tenzing also includes a Halcyon Thruster developed by Benchmark Space Systems. Halcyon is a monopropellant hydrogen peroxide propulsion system that will be used to maneuver the Tenzing spacecraft. The Halcyon is pressurized using an on-demand pressurization system which will prepare the thruster to be fired. The Halcyon thruster nozzle is placed in close alignment with Tenzing's center of gravity to avoid inducing significant rotation from the thruster firing.

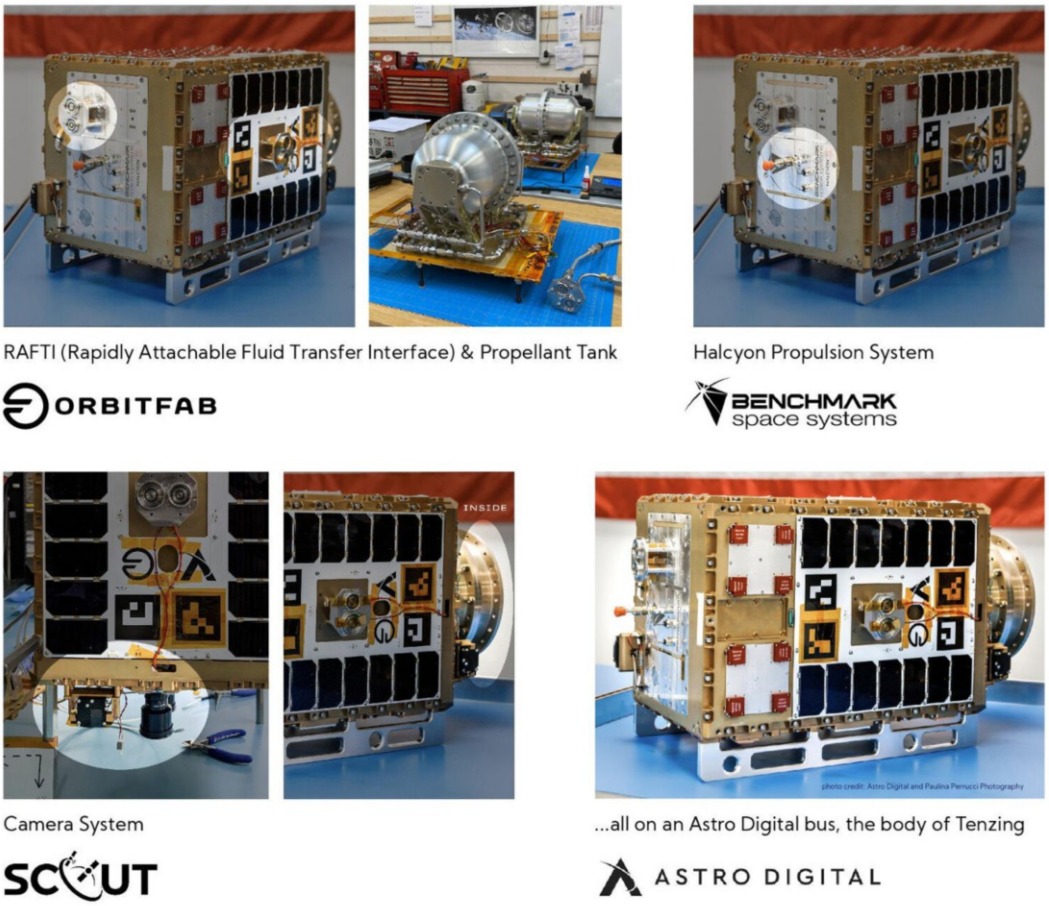

Figure 1. Tenzing Spacecraft with Key Subsystems Highlighted

RPO AS A SECONDARY MISSION

Proliferation of space assets within increasingly-crowded orbits increases the risk of any one satellite failing and consequently becoming dangerous space debris. The inclusion of OSAM into the equation promises both opportunities to reduce debris via controlled decommissioning and lifetime-extending missions, resolution of failure modes before space objects become debris, as well as new threats from potential failed servicing and other proximity operations.

OSAM operations and space-based infrastructure will not be able to scale effectively without commensurate scaling of numbers of RPO missions: RPO and failure mitigation capabilities have scaled only to deployments of dedicated RPO and servicing mission vehicles due to complexity and risk appetite. However, key missions in the past decade have showcased how smaller-scale, lower-cost subsystems enable these classically high-risk operations, such as the CanX-4 and -5 formation flight mission which demonstrated CubeSat-scale relative navigation to single-meter ranges at times[5]. Formation flight is a demonstration of dynamic station-keeping and proximity operations which shares many requirements with RPO, but has been demonstrated as a requirement in of itself for primary missions such as the Magnetospheric Multiscale Mission[6] (MMS). Range and uncertainty in drift due to attitude uncertainty is a driving factor in the risk of short-range RPO maneuvers[7], with two key potential means of being mitigated:

1. a means of inferring attitude of unsynchronized deputy vehicles for more accurate state propagation
2. direct state measurement between chaser and deputy on an ongoing basis, integrated with avoidance maneuver algorithms[iv]

The Tenzing mission implements SCOUT-Vision as a means of achieving the second means by measuring 3-degree-of-freedom states directly, which may be integrated into closed-loop navigation filters. The Tenzing mission is able to demonstrate direct measurement and decision-making with on-board COTS systems by Orbit Fab, Benchmark, and SCOUT. On-board sensing-enabled true autonomous decision-making, including *in situ* state estimation and reference truth during fly-by and RPO maneuvers is a step towards enabling more dynamic, proliferated operations in orbit.

FLY-BY TRAJECTORY DESIGN

Orbit Fab has partnered with Space Exploration Engineering (SEE) to develop an innovative, safe, and ΔV efficient flyby trajectory based on relative orbital element (ROE) targeting. The trajectory design for Tenzing's fly-by of Sherpa-FX2 leverages a co-elliptic rendezvous followed by eccentricity/inclination (E/I) vector separated near-field trajectory to ensure passive safety throughout the fly-by sequence (Figure 2). Natural in-track drift caused by differential drag drives in-track motion during the near-field phase of the fly-by. Ultimately, we target a 300 m x 140 m (crosstrack x radial) passive safety ellipse at the fly-by epoch to support the inspection imaging and relative navigation demonstration. Additionally, the trajectory provides regular hold points for propulsion system monitoring and relative navigation. Figure 2 provides an overview of the planned RPO con-ops and trajectory.

[iv] Within 2022 SCOUT vision system will demonstrate on-board, autonomous 6-DoF state estimation to de-risk short-range maneuvers; this will not be implemented onboard Tenzing.

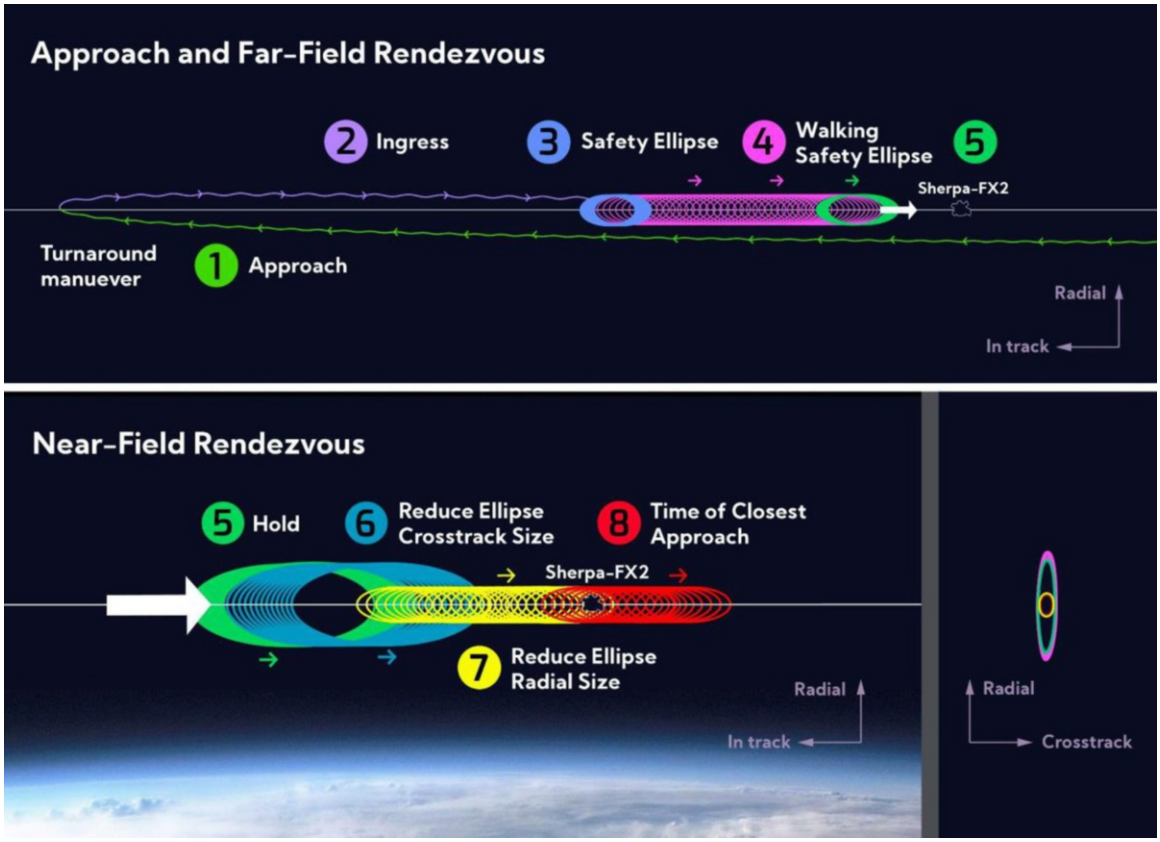

Figure 2. Tenzing - Sherpa-FX2 Flyby CONOPS Diagram

RPO Mission Sequence

We consider the mission design in four phases defined by the nature of the trajectory. Table 1 lists the approximate values of in-track separation and duration for each phase. Final values depend on the selected fly-by epoch.

Table 1. Fly-by phase summary with approximate in-track separation and duration

Phase	In-Track Separation		Duration	Trajectory
	Initial	*Final*		
Approach	-	+25 km	32 d	Co-elliptic rendezvous
Far-Field	+25 km	+10 km	6 d	1 km x 1 km* passive safety ellipse
Near-Field	+10 km	-10 km	5 d	300 m x 140 m* passive safety ellipse
Departure	-10 km	-	-	Co-elliptic departure

* PSE dimensions specified as crosstrack x radial, intrack dimension is twice the radial dimension

We use the quasi-nonsingular relative orbital elements (ROE) defined by D'Amico[8] to describe the trajectory design. In equation 1 and 2, we use the subscript d to note Tenzing's orbital elements

(the deputy spacecraft). Orbital elements with no subscript represent Sherpa-FX2, the chief or reference spacecraft.

$$\vec{\alpha} = \begin{pmatrix} a \\ u \\ e_x \\ e_y \\ i \\ \Omega \end{pmatrix} = \begin{pmatrix} a \\ \omega + M \\ e\cos\omega \\ e\sin\omega \\ i \\ \Omega \end{pmatrix} \tag{1}$$

$$\delta\vec{\alpha} = \begin{pmatrix} \delta a \\ \delta\lambda \\ \delta e_x \\ \delta e_y \\ \delta i_x \\ \delta i_y \end{pmatrix} = \begin{pmatrix} (a_d - a)/a \\ (u_d - u) + (\Omega_d - \Omega)\cos i \\ e_{x,d} - e_x \\ e_{y,d} - e_y \\ i_d - i \\ (\Omega_d - \Omega)\sin i \end{pmatrix} \tag{2}$$

We scale these non-dimensional ROE by the average semi-major axis of the reference satellite (Sherpa-FX2). Table 2 shows the ROE targets for each phase of the fly-by sequence.

Table 2. ROE for each fly-by phase [km]

Phase	$a\delta a$	$a\delta e_x$	$a\delta e_y$	$a\delta i_x$	$a\delta i_y$
Approach	*	0	0	‡	0
Far-Field	†	0	1	0	1
Near-Field	†	0	0.3	0	0.14
Departure	0.5	0	0	0	0

* Approach $a\delta a$ chosen to provide desired time-of-flight to far-field interface

† $a\delta a$ chosen to provide desired drift rate in presence of differential drag

‡ $a\delta i_x$ chosen to target desired $a\delta i_y$ at far-field interface by adjusting natural RAAN precession rate

These ROE targets will be adjusted based on propulsion system performance characterization from on-orbit testing before the flyby is executed.

Initial State

Tenzing and Sherpa-FX2 had a complex deployment sequence from the Falcon-9 second stage. Tenzing launched as a payload on the low-thrust Sherpa-LTE1 orbital transfer vehicle. After Sherpa-LTE1 separated from the second stage, Tenzing was deployed prior to any maneuvers being performed. Sherpa-FX2 separated from the Falcon 9 second stage in the opposite direction from Sherpa-LTE1. Neither Tenzing nor Sherpa-FX2 have performed any propulsive maneuvers since deployment. We perform regular orbit determination on both Tenzing and Sherpa-FX2 using radar

measurements from LeoLabs' network of ground radar stations. Table 3 lists the predicted ROE at the beginning of the fly-by operation.

Table 3. Initial ROE for fly-by operation based on latest OD solution [km]

$a\delta a$	$a\delta\lambda$	$a\delta e_x$	$a\delta e_y$	$a\delta i_x$	$a\delta i_y$
0.9721	-20833.6	-0.6234	-0.1794	0.1804	-7.1297

Note that this initial state corresponds to a relative mean argument of latitude of -172.7°. Once Tenzing exceeds half a revolution behind Sherpa-FX2, the sign of $a\delta\lambda$ flips. Table 4 lists the predicted Keplerian orbital elements for Sherpa-FX2 when the fly-by operation begins.

Table 4. Initial mean Keplerian orbital elements for fly-by operation based on latest OD solution [km, deg]

a	e	i	Ω	ω
6890.47	0.0043	97.52	191.28	109.78

Approach

Tenzing uses a co-elliptic approach to begin the rendezvous with Sherpa-FX2. This approach strategy ensures passive safety by providing a radial offset at zero in-track separation. Burn pairs target the desired in-plane ROE ($a\delta a$, $a\delta e$). By setting $a\delta e$ = 0, the line of apsides of Tenzing's and Sherpa-FX2's orbits are aligned to prevent potential conjunctions. The relative semimajor axis ($a\delta a$) sets the desired time-of-flight. Figure 3 shows the co-elliptic approach in the $a\delta a$-$a\delta\lambda$ phase space. Sherpa-FX2 is located at the origin. This approximates in-plane motion in the curvilinear RIC reference frame. The green star indicates the initial point and the red diamond the final state.

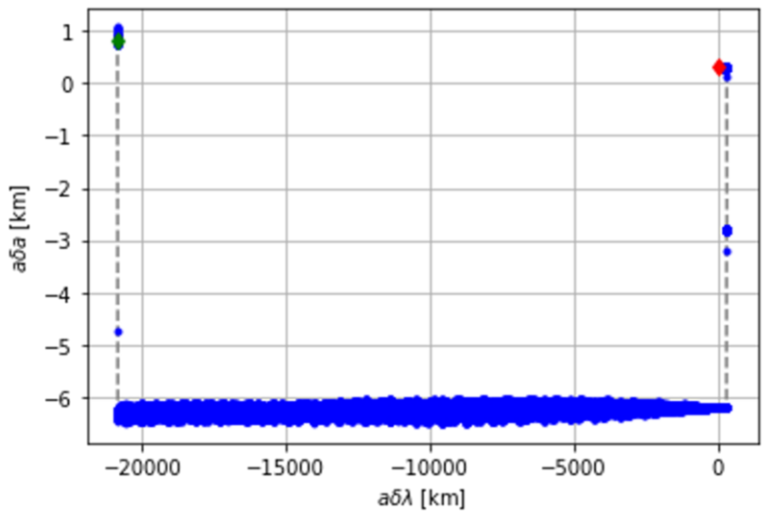

Figure 3. Tenzing approach phase leverages a co-elliptic rendezvous

Figure 4 shows the initial fly-by of Sherpa-FX2 with passive safety provided by radial separation. The approach phase always delivers Tenzing to a final state ahead and above Sherpa-FX2. This ensures that differential drag will naturally decrease the range between Sherpa-FX2 and Tenzing. Additionally, prior to near- and far-field rendezvous, differential drag will lead to increasing radial separation in the absence of maneuvers.

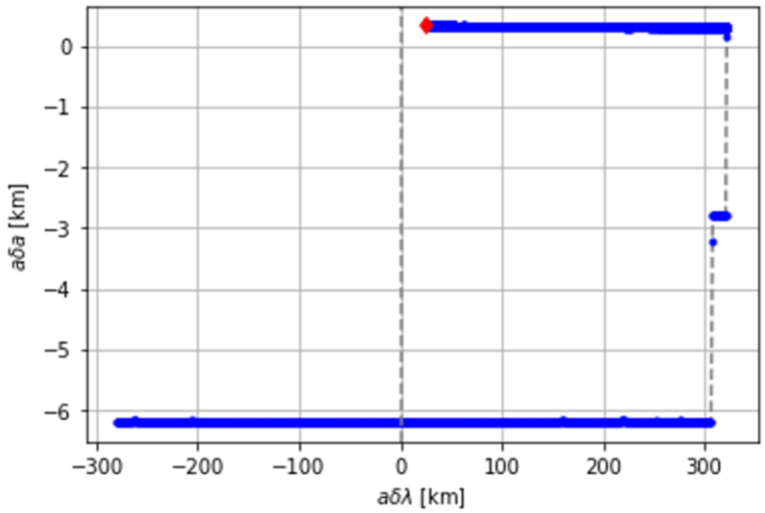

Figure 4. Co-elliptic approach provides passive safety by radial separation at initial fly-by

Figure 5 verifies that Tenzing's co-elliptic approach minimizes relative eccentricity during the inbound drift phase. With a maximum $|a\delta \boldsymbol{e}| < 700m$, we are assured that the maximum radial excursion during the first fly-by will be less than 1 km, maintaining over 5 km of radial separation. Figure 5 presents the magnitude of the relative eccentricity during the planned maneuver.

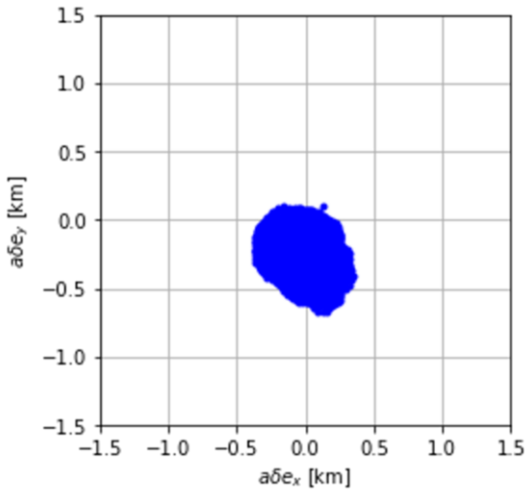

Figure 5. Near-zero relative eccentricity during co-elliptic approach provides passive safety with radial offset shown in figure 4

In addition to in-track phasing, the approach phase must manage relative RAAN ($a\delta i_y$) in order to ensure the required out-of-plane maneuvers to enter the initial passive safety ellipse are of a reasonable magnitude. At its lower initial orbit, Sherpa-FX2 experiences a higher rate of RAAN

precession than Tenzing. In order to correct this, Tenzing approaches Sherpa-FX2 in a prograde direction ($a\delta a < 0$). Since Tenzing is now in the lower orbit, it will experience a higher RAAN precession rate than Sherpa-FX2. We select the specific value of $a\delta a$ for the approach phase to achieve a time-of-flight of ~30 days. Tenzing performs a small out-of-plane maneuver early in the approach to fine-tune relative RAAN drift (once $a\delta a$ is set) and target the desired $a\delta i_y$ at far-field interface. Since relative RAAN ($a\delta i_y$) is sensitive to both relative semi-major axis ($a\delta a$) and relative inclination ($a\delta i_x$), controlling both during approach allows Tenzing to achieve the desired both the desired in-track position ($a\delta\lambda$) and out-of-plane phasing ($a\delta i_y$) within the desired time-of-flight. Figure 6 shows the drift in both $a\delta i_x$ and $a\delta i_y$ during the approach phase. The elapsed days used here and in subsequent figures are referenced to the beginning of the approach phase.

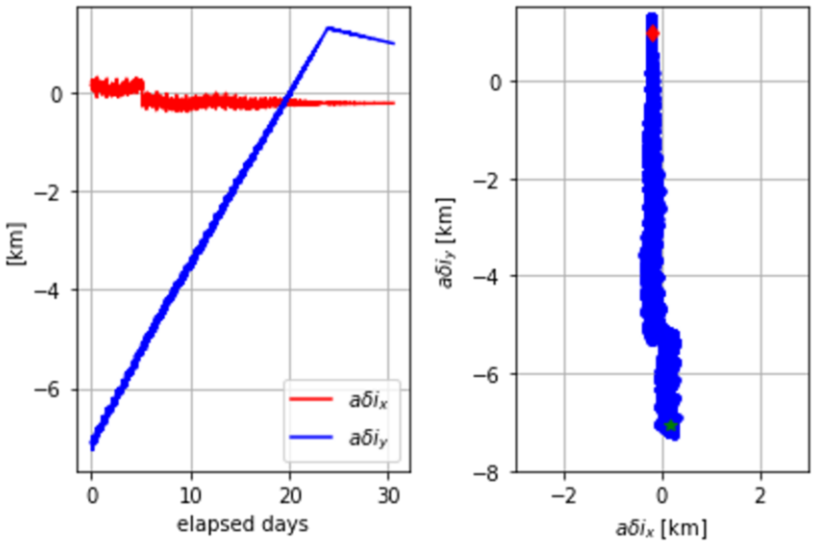

Figure 6. Approach phase uses relative semi-major axis and small relative inclination to adjust relative RAAN for PSE insertion. Inclination vector evolution shown as timeseries (left) and in inclination plane (right).

Far- and Near-Field RPO

The far- and near-field RPO phase is characterized by a steady approach towards Sherpa-FX2 driven by differential drag. In general, Tenzing does not actively control its in-track position, relying on the timing of each transition maneuver to periodically adjust the rate of approach. Table 5 lists the sequence of events surrounding the fly-by.

Table 5. Far- and near-field RPO sequence of events, dashed line indicates far/near field interface

Seq	Event	Start $a\delta\lambda$ [km]	Stop $a\delta\lambda$ [km]	Duration [d]
1	Insert into 1 km x 1 km PSE	+25	+19.6	1.11
2	3 day hold	+19.6	+13.7	3.00
3	Ingress in 1 km x 1 km WSE	+13.7	+9.6	1.00
4	1 day hold	+9.6	+9.3	1.00

5	Transition to 300 m x 140m PSE	+9.3	+3.7	3.04
6	Ingress in 300 x 140 m WSE	+3.7	0	1.77
7	Egress in 300 x 140 m WSE	0	-10	2.68

The far-field RPO trajectory begins with Tenzing inserting into a 1 km x 1 km passive safety ellipse. In this configuration, the eccentricity and inclination vectors are aligned such that the maximum crosstrack separation coincides with the minimum radial separation and vice-versa. As a result, large in-track uncertainties do not pose a risk of collision since Tenzing is never directly on Sherpa-FX2's extended orbit track. Figure 7 shows Tenzing's trajectory in $a\delta a$ - $a\delta\lambda$ phase space. The red numbers correspond to the sequence IDs in table 5.

The step-wise discontinuities at points 1 and 3 correspond to eccentricity reconfiguration maneuvers. The drift during these maneuvers is caused by the relative semi-major axis during the transfer orbit. The inverted wedge shaped discontinuity at point 5 represents an eccentricity reconfiguration where Tenzing actively maintains its in-track position. Due to the close proximity to Sherpa-FX2 and the large eccentricity change between the 1 km x 1 km and 300 m x 140 m PSE, we control Tenzing's in-track position ($a\delta\lambda$) during this reconfiguration to avoid reaching Sherpa-FX2 prematurely. In-track drift is permitted in the reconfigurations at points 1 and 3 in order to reduce required maneuver ΔV.

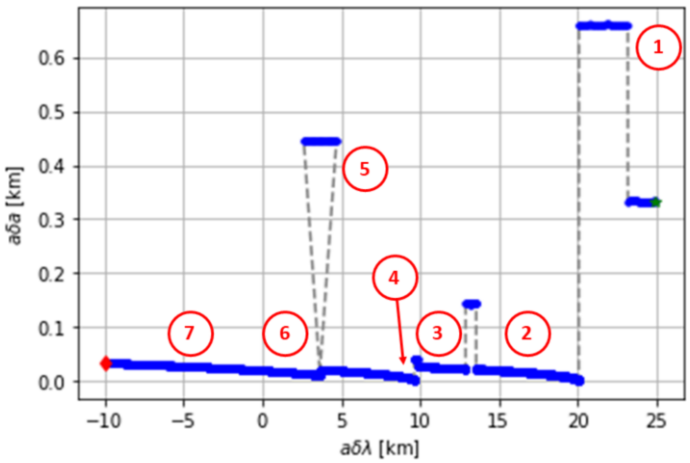

Figure 7. In-plane ROE during far- and near-field RPO

Figure 8 shows Tenzing's far- and near-field trajectory in the eccentricity and inclination planes. The E/I vectors are considered parallel since both have their x-components at (or near) zero and a positive y-component. The parallel configuration of the E/I vectors ensures passive safety throughout the trajectory. The deviations in the eccentricity plot are transient perturbations to the eccentricity vector during reconfiguration maneuvers. The initial offset in the inclination vector is due the small $a\delta i_x$ used to fine tune relative RAAN during the approach phase. This is removed during the insertion maneuvers for the initial 1 km x 1 km PSE.

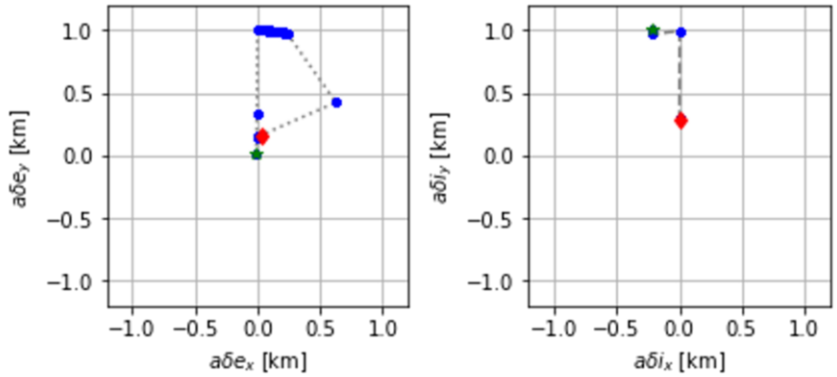

Figure 8. Eccentricity (left) and inclination (right) vector plots for far- and near-field RPO, green star indicates initial state, red diamond indicates final state

Figure 9 shows Tenzing's far- and near-field trajectory in the radial-intrack-crosstrack reference frame centered on Sherpa-FX2. The green stars indicate the initial position and the red diamond the final position.

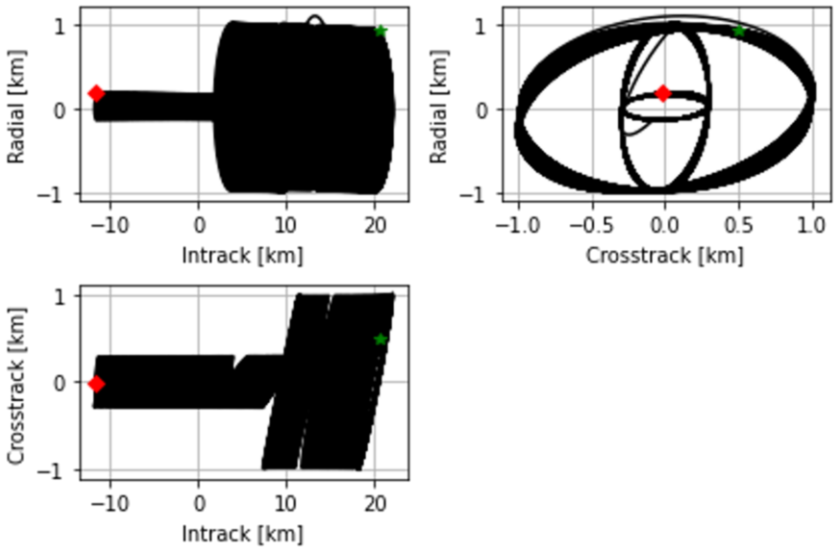

Figure 9. Fly-by trajectory in the Sherpa-FX2 centered RIC reference frame

Departure

By designing the far- and near-field RPO phases to leverage the natural drift due to differential drag, Tenzing is assured safe departure from the vicinity of Sherpa-FX2 even in the absence of a "getaway maneuver". The fly-by trajectory design includes a final burn pair after the fly-by to transition Tenzing into a co-elliptic orbit with Sherpa. As with the approach phase, this eliminates periodic radial/intrack motion and reduces the risk of collision through radial separation. The departure maneuver targets $a\delta a = 500\,m$. Differential drag will naturally increase this radial separation over time, minimizing conjunction risk between Sherpa-FX2 and Tenzing.

Principles of Safe RPO Maneuvers

Tenzing's flyby trajectory is designed with safety as a primary consideration. At all times during the rendezvous, Tenzing will be passively safe through its no-burn trajectory not

intersecting the track of Sherpa FX-2. Tenzing's Vbar approach will be done using Walking Safety Ellipses (WSE). A WSE uses parallel vectors of relative eccentricity ($\Delta\mathbf{e}$) and relative inclination ($\Delta\mathbf{i}$) to achieve natural motion circumnavigation of the client vehicle the radial (achieved by $\Delta\mathbf{e}$) and cross track (achieved by $\Delta\mathbf{i}$) plane[8].

The minimum dimensions of the final ellipse during near-field rendezvous will be sized based on the 3-sigma uncertainty in the relative covariance between Tenzing and Sherpa FX-2 in the radial and cross track axes, propagated for duration of time between the final maneuver and the TCA.

The flyby will be de-risked by performing a series of ground and on-orbit tests. All scripts to be delivered to Tenzing will be tested on a Flat Sat prior to uplink. The ground to ground communications, data delivery chain, and Tenzing's attitude control will be tested by slewing the spacecraft as if for an out of plane maneuver prior to the first burn. Prior to the first co-elliptic flyby maneuver, the Halcyon thruster will be test fired; this will also help the team characterize the thruster performance in orbit.

Tenzing's no-burn safe trajectory is verified by removing the maneuver at the beginning of Far-Field Rendezvous, the insertion into a 1km by 1km passive safety ellipse. 13.6 hours after the missed burn Tenzing will make an Rbar crossing of Sherpa-FX2, 300m above in the radial direction, presented in Figure 10. Since deployment in July 2021, the differential drag between the two spacecraft has caused Sherpa-FX2's semi-major axis to decrease at a faster rate than Tenzing's. In this no-burn scenario, differential drag would cause the radial separation at consecutive Rbar crossings to increase.

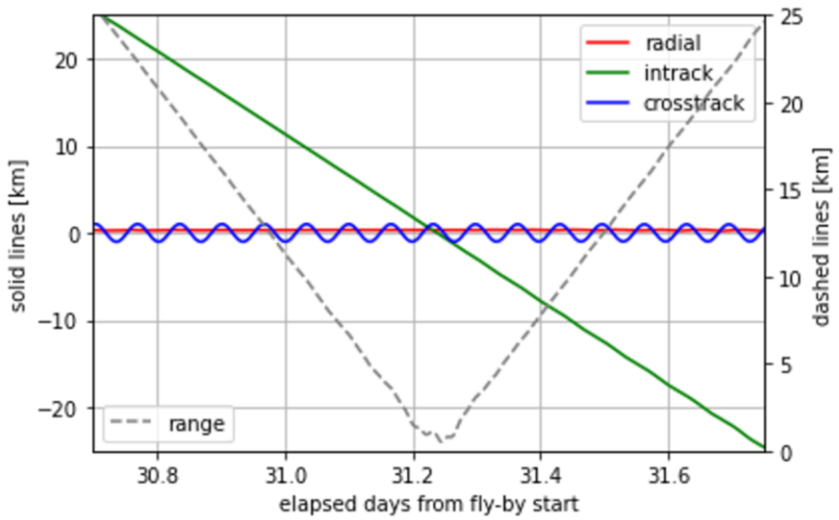

Figure 10. RIC coordinate representation of the Rbar crossing.

MANEUVER DESIGN PROCESS

The maneuver design process for Tenzing's fly-by trajectory leverages the closed form control algorithm developed by D'Amico and Montenbruck[9] combined with simple differential-correctors for final targeting. For in-plane reconfiguration, we use two impulses along and opposite the tangent to the orbit. Since Tenzing is in a near-circular orbit, we use the approximate $v = na$ to write the control algorithm in terms of the dimensional ROE, for convenience. Equation 3 defines the magnitudes and locations (in terms of mean argument of latitude) of these two burns for desired changes in $a\delta a$ and $a\delta e$.

$$\begin{aligned}
\Delta v_T^1 &= +\frac{n}{4}\left(\sqrt{\Delta \mathrm{a}\delta e_x^2 + \Delta \mathrm{a}\delta e_y^2} + \Delta \mathrm{a}\delta \mathrm{a}\right) \\
\Delta v_T^2 &= -\frac{n}{4}\left(\sqrt{\Delta \mathrm{a}\delta e_x^2 + \Delta \mathrm{a}\delta e_y^2} - \Delta \mathrm{a}\delta \mathrm{a}\right) \\
u^1 &= \operatorname{atan}\left(\frac{\Delta a \delta e_y}{\Delta a \delta e_x}\right) \\
u^2 &= u^1 + \pi
\end{aligned} \tag{3}$$

For out-of-plane reconfiguration, we use a single impulse along the orbit normal. Equation 4 defines the magnitude and location of this single burn.

$$\begin{aligned}
\Delta v_N &= n\sqrt{\Delta a \delta i_x^2 + \Delta a \delta i_y^2} \\
u &= \operatorname{atan}\left(\frac{\Delta a \delta i_y}{\Delta a \delta i_x}\right)
\end{aligned} \tag{4}$$

We use the Astrogator tool in AGI's Systems ToolKit (STK) for trajectory design and maneuver planning. The quasi-nonsingular ROE are implemented as custom calculation objects for use in Astrogator's targeting algorithms. Maneuvers are initially designed as impulsive burns. The initial value for the magnitude and location of each burn is calculated using the closed form control algorithm described above. A differential-corrector then refines the maneuver magnitude, pointing, and/or location to precisely achieve the desired ROE. Finally, we seed finite maneuvers from the impulsive solution and use a differential-corrector to refine the finite maneuver design to achieve the same target ROE.

As a capability-driven mission, we expect to incrementally gain better understanding of the propulsion system performance as the mission progresses beyond the initial thruster calibration. The approach maneuvers are least sensitive to maneuver execution errors and can tolerate a greater degree of uncertainty. The PSE reconfiguration maneuvers immediately prior to the fly-by are most sensitive and occur after 12 operational burns for further thruster performance assessment. During the far- and near-field phase, maneuvers occur at cadence sufficient for correcting errors introduced by navigation and maneuver execution errors. The dimensions of the final PSE were selected to tolerate the expected navigation errors and can be adjusted if maneuver execution errors are larger than expected.

Prior to each major reconfiguration, a go/no-go poll will be conducted to verify that the spacecraft and team are ready to proceed with the planned maneuvers. The trajectory has been designed such that, in the event of a "no-go", the spacecraft will remain passively safe in the absence of the next planned maneuver. Figure 11 shows three example trajectories with maneuvers omitted. In every case, Tenzing remains clear of the vicinity of Sherpa-FX2.

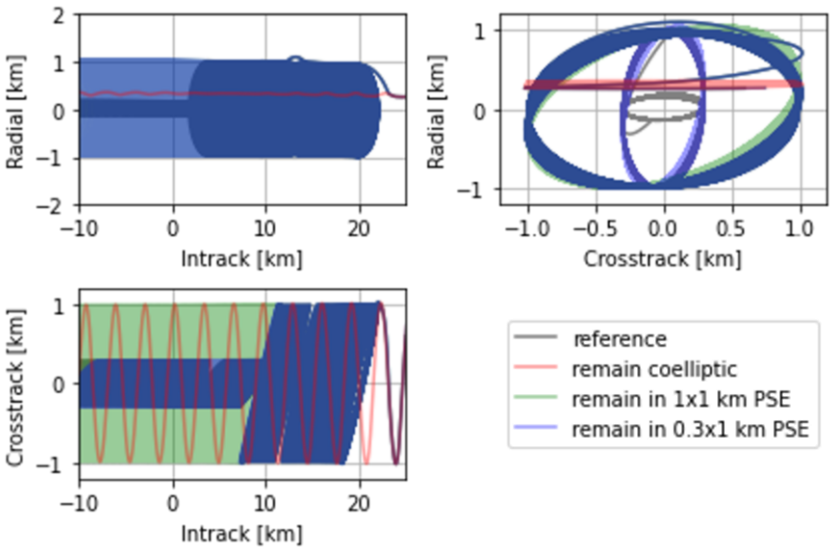

Figure 11: Missed maneuver trajectories demonstrate robustness

Relative Navigation

Throughout the close proximity phase of the operation, Tenzing will utilize its onboard SCOUT-Vision payload to collect and process images of Sherpa. The payload computer ties the stereoscopic optics and on-board telemetry together to provide comprehensive state estimation of nearby objects. Figure 12 presents a simulated scenario produced by system-in-loop testing with an emulated sensor and a simulated synthetic environment.

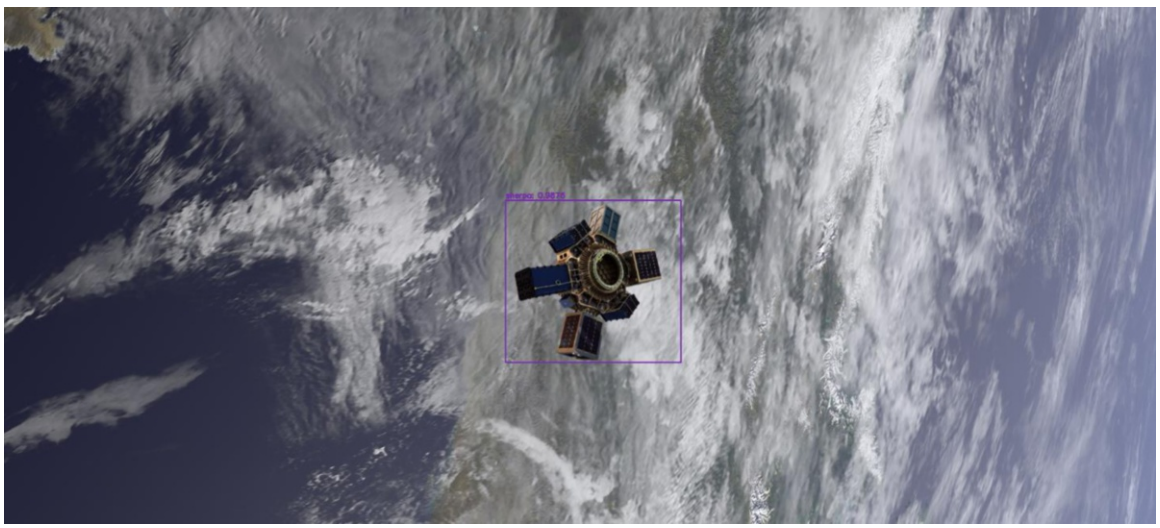

Figure 12. Synthetically-generated Spaceflight Sherpa OTV identified and located in a space environment at range, emulating sensors and algorithms flying on Tanker-001.

Sensor operations will be integrated to enable more autonomous close-range RPO, and derivative data products will provide data for control algorithms. Direct metric measurements, for closed-loop on-board relative navigation between a chaser such as Tenzing and a deputy such as the Sherpa-FX2, will provide unprecedented accuracy in ranging between chaser and deputy, which may drive avoidance in risky scenarios otherwise not positively identifiable from the Earth. Fine optical sensor-based relative state estimation will begin with Tenzing in near-field operations

within an in-track range of 5 km, and showcase state-of-the-art inter-satellite imaging at significant ranges for small satellite architectures[10].

The Tenzing mission, leveraging its onboard SCOUT-Vision stereo optics and corresponding software, will directly measure the Sherpa spacecraft's state during the various phases of the RPO maneuver using on-board computer vision algorithms. These algorithms use convolutional neural networks to determine observed object identification and position in relation to the observer, providing, on Tenzing, 3-degree-of-freedom state measurements on a continuous basis to a navigation filter. From relative states, relative state rates are calculated, and within a short-range rendezvous the spacecraft can track propagated and estimated state rates to track discontinuities or drift.

The navigation filter is built upon an unscented Kalman filter,and provides key absolute knowledge on drift in particular. This is presented in Figure 13, with the navigation filter mitigating propagated drift velocity error following a sensor outage within the walking safety ellipse at a range of ~300 meters.

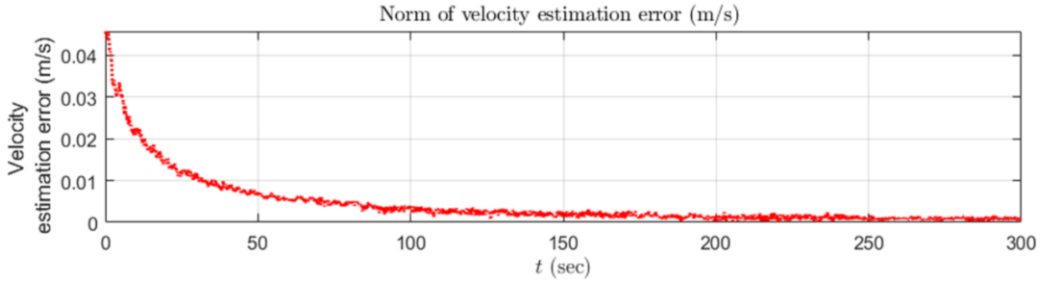

Figure 13. Simulated state estimation normal velocity error and drift response timeline following a sensor outage scenario within the ingress stage of the RPO.

Optical-based relative navigation such as that integrated on the Tenzing mission can provide high-precision measurement of the relative state between spacecraft on an ongoing basis. Integrating a closed-loop navigation filter, to better manage the data inflow such as that of the SCOUT-Vision systems and other sensors aboard Tenzing, provides a demonstration of more ground command-agnostic, and consequently more autonomous, de-risking of RPO maneuvers.

CONCLUSION

This flyby activity and the architectures enabling it are a step towards meeting the RPO needs of future OSAM missions. Orbit Fab and SEE have exemplified safe rendezvous practices through the use of passively safe ellipses that do not intersect the track of Sherpa-FX2 and will not lead to a conjunction regardless of any missed maneuvers. Tenzing's ingress is radially separated and passively safe due to differential drag. Far and Near-Field Rendezvous use walking safety ellipses targeted using relative orbital elements and sized larger than the 3 sigma relative uncertainty from orbit determination. The Tenzing - Sherpa-FX2 flyby will demonstrate the ability of small satellites to execute RPO using COTS components and without being designed towards such capabilities as a primary mission objective. Following completion of the flyby, images of Sherpa-FX2 will be downlinked and definitive ephemerides surrounding the flyby can be generated. The results of this flyby operation will reduce risk for future OSAM missions, particularly those under development by Orbit Fab and SCOUT. In particular, heritage from this flyby will be key for implementing RPO and docking using Orbit Fab's RAFTI docking and refueling interface on missions to be launched over the course of the next few years.

ACKNOWLEDGMENTS

The authors would like to thank Astro Digital and the Tenzing ops team for making the mission and the flyby possible. Thanks to Benchmark Space Systems for providing the Halcyon thruster and continued support throughout the mission. The team thanks Spaceflight Industries for Tenzing's transport aboard the Sherpa LTE-1 and the ability to demonstrate our rendezvous and proximity operations with Sherpa-FX2. Additional thanks to Anna Shaposhnik of Orbit Fab for creation of the flyby CONOPS diagram.

REFERENCES

1. O'Leary, A., Burkhardt, Z., Bultitude, J., Faber, D., and Schiel, J. "Refueling Architectures for VLEO Missions." *DISCOVERER.* Poster. 2021.

2. Schiel, J., Faber, D., Bultitude, J., Yang, K., "How On Orbit Fueling Supports the Deorbit Tug Business Case" *Proceedings of the International Astronautical Congress,* Washington, DC, USA. 2019

3. Bultitude, J., Burkhardt Z., Harris, M., Jelderda M., Suresh, S., Fettes, L., Faber, D., Schiel, J., Cho, J., Levitt, D., Kees, D., Gallucci, S., "Development and Launch of the World's First Orbital Propellant Tanker." *Proceedings of the Small Satellite Conference*, Logan, UT. 2021.

4. Bultitude, J., Suresh, S., Deuitch, A., Cho, J., Fettes, L., Burkhardt, Z., O'Leary, A., Harris, M., Jelderda, M., Faber, D., Schiel, J., Kendall-Bell, G., "First Flight of RAFTI Orbital Refueling Interface." *Proceedings of the International Astronautical Congress,* Dubai, UAE. 2021.

5. Bonin, G., Roth, N., Armitage, S., Risi, B. and Zee, R. "The CanX-4&5 Formation Flying Mission: A Technology Pathfinder for Nanosatellite Constellations." *Proceedings of the Small Satellite Conference*, Logan, UT. 2013.

6. Fuselier, S.A., Lewis, W.S., Schiff, C., Ergun, R., Burch, J.L., Petrinec, S.M. and Trattner, K.J., "Magnetospheric multiscale science mission profile and operations." *Space Science Reviews*, 199(1), pp.77-103. 2016.

7. Lee, D., and Vukovich, G. "Kinematically coupled spacecraft relative motion without attitude synchronization assumption." *Aerospace Science and Technology 45,* pp.316-323. 2015.

8. S. D'Amico. "Autonomous Formation Flying in Low Earth Orbit. Delft University of Technology." *Doctoral Dissertation,* TU Delft. 2010.

9. D'Amico, S. and Montenbruck, O. "Proximity operations of formation-flying spacecraft using an eccentricity/inclination vector separation." *Journal of Guidance, Control, and Dynamics*, 29(3), pp.554-563. 2006.

10. Gangestad, J.W., Venturini, C.C., Hinkley, D.A. and Kinum, G. "A Sat-to-Sat Inspection Demonstration with the AeroCube-10 1.5 U CubeSats." *Proceedings of the Small Satellite Conference*, Logan, UT. 2021.